

SUPPLEMENTAL INFORMATION

Jayaraman S. et al.

Materials and Methods

Proteins and lipids Recombinant murine SAA isoform 1 (mSAA1, 103 a. a., 11.6 kDa) was expressed in *E-coli* and purified to 95% purity as described previously.¹ Lipids 1-palmitoyl-2-oleoyl-*sn*-glycero-3-phosphocholine (POPC, C16:0, C18:1), 1-palmitoyl-2-oleoyl-*sn*-glycero-3-phosphoethanolamine (POPE, C16:0, C18:1), 1-palmitoyl-2-oleoyl-*sn*-glycero-3-phospho-(1'-*rac*-glycerol) (POPG C16:0, C18:1) and chicken egg sphingomyelin (SM, C16:0) were 97 %+ pure from Avanti Polar Lipids. Ultrapure fluorescence probe thioflavin T (ThT), trypsin from bovine pancreas (cat. # T1426), secretory phospholipase A₂ from honey bee venom, sPLA₂III (cat. # 9279), and sodium oleate 99%+ pure (cat. # O7501) were from Sigma. EnzyChrom™ free fatty acid assay kit (EFFA-100) and EnzyChrom™ phospholipid assay kit (EPLP-100) from original vendors BioAssay system were from Fisher Scientific. Ultrapure sodium phosphate buffer at pH 7.5 (BB-148) and 5 M sodium chloride solution (BM-244) were from Boston Bioproducts. All other chemicals were of highest purity analytical grade. Protein stock solutions were prepared by dissolving lyophilized SAA at 1 mg/ml in water and dialyzed against standard buffer (50 mM sodium phosphate, 150 mM NaCl, pH 7.5) overnight. Protein stock solution was centrifuged at 10,000 g for 10 min prior to each experiment to remove protein aggregates.

SAA complexes with lipids or free fatty acid and lipid clearance assay Multilamellar vesicles (MLVs) of POPC, POPE, POPG and SM were prepared by dissolving the lipid in chloroform:methanol (2:1 v/v); the organic solvent was evaporated under nitrogen stream, and the samples were dried under vacuum overnight at 4 °C to ensure complete solvent removal. MLVs were prepared by dispersing the lipid films in 50 mM sodium phosphate buffer containing 150 mM NaCl, pH 7.5, followed by vigorous vortexing. SAA was incubated at 25 °C for 3 h with MLVs at protein:lipid molar ratio ranging from 1:1 (low lipid) to 1:100 (high lipid). Uncomplexed lipid and protein were removed by centrifugation and gel filtration, respectively.

Potential effects of the initial oligomeric state of free SAA on its lipidation were analyzed in lipoprotein reconstitution experiments by varying one parameter at a time: (i) SAA concentrations of 0.02-1.0 mg/ml, which influence protein self-association²; (ii) temperature of lipoprotein reconstitution (4, 25 or 37 °C), which affects the secondary structure and self-association of SAA³; (iii) incubation of free SAA at 70 °C for 15 min to dissolve protein oligomers immediately prior to the addition of lipid; and (iv) using 3 M urea, which dissociates SAA oligomers into monomers⁴.

The SAA:lipid complexes formed in these experiments had very similar stoichiometry and size distribution, suggesting that oligomerization of free SAA had no significant effect on the lipoprotein assembly. The effects of pH on the SAA oligomer structure and lipidation was addressed on our recent study showing that lysosomal pH greatly reduced the formation of lipoprotein particles above 8 nm in size⁵.

MLV clearance by SAA at room temperature was monitored by turbidity at 325 nm using a Varian Cary-300 UV-vis spectrophotometer. SAA (20 µg/ml) was rapidly mixed with MLV suspension in standard buffer (40 µg/ml lipid), and the time course of turbidity changes was recorded as large micron-size MLVs were converted into smaller lipoprotein nanoparticles. MLVs alone (without protein) were used as controls; Fig. 1A shows representative data for POPC MLVs; controls using MLVs of other lipids (not shown to avoid overlap) were very similar.

To prepare SAA complexes with oleic acid (OA), SAA (0.5 mg/ml) was incubated with freshly prepared emulsion of sodium oleate (5 mmol) in standard buffer for 2 h at 37 °C.

Phospholipid hydrolysis by PLA₂ and assays for free fatty acid and phospholipids
SAA:lipid complexes containing 0.5 mg/ml protein were dialyzed against 10 mM Tris buffer containing 150 mM NaCl, pH 7.5. Next, the complexes were hydrolyzed with 50 nm recombinant bee-venom sPLA₂-III in Tris buffered saline, pH 7.4, containing 2 mM CaCl₂. After 3 h incubation at 37 °C the lipolysis was terminated by adding EDTA to a final concentration of 20 mM. The extent of phospholipid hydrolysis was assessed by measuring the amount of released free fatty acids using free fatty acid assay kit (EnzyChrom™).

Free fatty acid and total phospholipids were quantified using kits from BioAssay systems following manufacturer's instructions. All assays were done in technical triplicates and were repeated in biological triplicates.

Gel electrophoresis and gel filtration For non-denaturing polyacrylamide gel electrophoresis (PAGE), Novex™ 4-20% Tris-glycine gels (Invitrogen) were loaded with 6 µg protein per lane and run to termination at 1,500 V·h under non-denaturing conditions in Tris-glycine buffer. For SDS PAGE, Novex™ 18% Tris-glycine gels were loaded with 5 µg protein per lane and run at 200 V for 1 h under denaturing conditions in SDS-Tris-glycine buffer. The gels were stained with Denville Blue protein stain (Denville Scientific).

Size exclusion chromatography was performed with a Superdex 75 10/300 GL column (GE Healthcare) controlled by an ÄKTA UPC 10 FPLC system (GE Healthcare). Elution by phosphate

buffer saline (50 mM sodium phosphate, 150 mM NaCl, pH 7.5) was carried out at a flow rate of 0.5 ml/min.

Circular dichroism (CD) spectroscopy CD data were recorded using an AVIV 62 spectropolarimeter to monitor protein secondary structure and thermal stability. Far-UV CD spectra were recorded at 190-250 nm from solutions containing 0.1 mg/ml SAA in standard buffer. Melting data were recorded at 222 nm to monitor α -helical unfolding during sample heating and cooling at a constant rate of 70 °C/h. Selected melting data were recorded at a rate of 10 °C/h and showed no scan rate effects. Buffer baselines were subtracted from the data and the results were normalized to the protein concentration and reported as molar residue ellipticity, $[\Theta]$, in units of $1000 \cdot \text{deg} \cdot \text{cm}^2 \cdot \text{dmol}^{-1}$.

Limited proteolysis and mass spectrometry SAA, either in lipid-free form or in complexes with lipids, was incubated with trypsin at 1:1500 mg:mg enzyme:substrate ratio in standard buffer at room temperature. Tryptic digestion was quenched using 2 mM of a serine protease inhibitor phenylmethylsulfonyl fluoride. The reaction was quenched after 5 min in lipid-free SAA, which was rapidly digested, and after 1 h for lipid-bound forms, which were digested much more slowly. The reaction products were analyzed by SDS page and matrix-assisted laser desorption ionization – time of flight (MALDI-TOF).

For MALDI-TOF, the spectra were recorded on a Reflex-IV spectrometer (Bruker Daltonics, Billerica, MA) equipped with a 337 nm nitrogen laser. The instrument was operated in the positive-ion reflection mode at 20 kV accelerating voltage with time-lag focusing enabled. Calibration was performed in linear mode using a standard calibration mixture containing oxidized B-chain of bovine insulin, equine cytochrome C, equine apomyoglobin, and bovine serum albumin. The matrix, cyano-4-hydroxycinnamic acid (alpha cyano, $M_w=189$ g/mol), was prepared as a saturated solution in 70% acetonitrile and 0.1% trifluoroacetic acid in water. Mass spectrometry results were reported as an average of three independent experiments. The error in the molecular mass determination is ± 15 Da.

Transmission electron microscopy For transmission electron microscopy (TEM), protein stock solutions were diluted to 0.1 mg/ml SAA and a 4 μl clear drop was deposited onto grids. Fibril-containing samples were centrifuged and the clear solution was deposited onto grids. The grids were washed with double-distilled water and stained with 1% uranyl acetate. Electron micrographs were collected under low-dose conditions at a 45,000 magnification using a CM12 transmission electron microscope (Philips Electron Optics, the Netherlands) equipped with a Teitz 2K x 2K CCD camera (TVIPS, Gauting, Germany).

Amyloid formation SAA (1 mg/ml in standard buffer) was incubated at 37 °C without shaking for up to 80 h. Sample aliquots were taken at different time points for further studies. Formation of amyloid-like structure was monitored using a thioflavin T (ThT) fluorescence emission, which increases upon binding to amyloid. ThT was added to protein aliquots (10 μM SAA) at a final dye concentration of 20 μM, which was determined spectrophotometrically at 412 nm using extinction coefficient of 36,000 M⁻¹·cm⁻¹. ThT emission spectra at 25 °C were collected at 450-550 nm using $\lambda_{\text{ex}}=440$ nm with 5 nm excitation and emission bandwidths. The emission spectrum of ThT in buffer was subtracted from the data. The ThT emission intensity was determined by peak integration from 450 nm to 500 nm, and the integrated intensity was plotted as a function of time. Each experiment was performed in quadruplicate. As a control, ThT was incubated at 37 °C with lipid vesicles alone (1000 μM lipid) or with 5 mM sodium oleate, and the emission was recorded for up to 80 h; no significant emission changes were detected. Therefore, the increase in emission observed during protein fibrillation resulted from ThT binding to the protein rather than lipid.

After 72 h incubation, sample aliquots were analyzed by TEM for amyloid fibril formation.

To ensure reproducibility, all experiments in this study were repeated four or more times; all gel electrophoresis data were repeated five times.

Supplemental Tables

Lipid / curvature	Chemical structure
1-palmitoyl-2-oleoyl-sn-glycero-3-phosphocholine (POPC) Spontaneous curvature: 0	
1-palmitoyl-2-oleoyl-sn-glycero-3-phospho-ethanolamine (POPE) Spontaneous curvature: <0	
1-palmitoyl-2-oleoyl-sn-glycero-3-phospho-(1'-rac-glycerol) (POPG) Spontaneous curvature: 0	
Sphingomyelin (SM) Spontaneous curvature: ≥0 depending on the head group	
16:0 Lyso-PC Spontaneous curvature: >0	
16:0 Lyso-PE Spontaneous curvature: >0	
16:0 Lyso-PG Spontaneous curvature: >0	
Oleic acid (OA) Spontaneous curvature: <0	$\text{CH}_3(\text{CH}_2)_6\text{CH}_2\text{CH}=\text{CH}(\text{CH}_2)_7\text{COOH}$

Table S1. Chemical structures of lipids relevant to the current study. The structures were taken from Avanti Polar Lipids website (<https://avantilipids.com/>).

Phospholipid	Final High lipid mg/ml ± 0.005	Final High lipid μM	Final Low lipid mg/ml ± 0.005	Final Low lipid μM	α-helix % ± 5%	
					High lipid	Low lipid
POPC	0.21	270	0.01	13	56.4	24.5
POPE	0.14	193	0.03	41	55.4	35.2
POPG	0.11	140	0.03	38	55.6	33.5
SM	0.65	910	-	-	51.2	17.6

Table S2. Biochemical and structural characterization of SAA complexes with phospholipids. The initial amount of SAA in all preparations was 0.5 mg/ml (43 μM). For the “high-lipid” preparations the initial lipid concentration was 3.3 mg/ml (1:100 protein:lipid mol:mol) and for the “low-lipid” preparations it was 0.035 mg/ml (1:1 protein:lipid mol:mol). SAA was incubated with lipids for 3 h at 37 °C. Excess lipids were removed by centrifugation and excess protein was removed by gel filtration as previously described.² Phospholipids were quantified by using an assay kit as described in Methods. The tabulated numbers represent an average of three independent measurements and the standard error of mean. For the “low-lipid” SAA complexes with SM, the quantity of lipid was below the estimation limit. The α-helical content was estimated based on the molar residue ellipticity at 222 nm measured by CD spectroscopy as previously described with 5% accuracy.²

Supplemental Figures

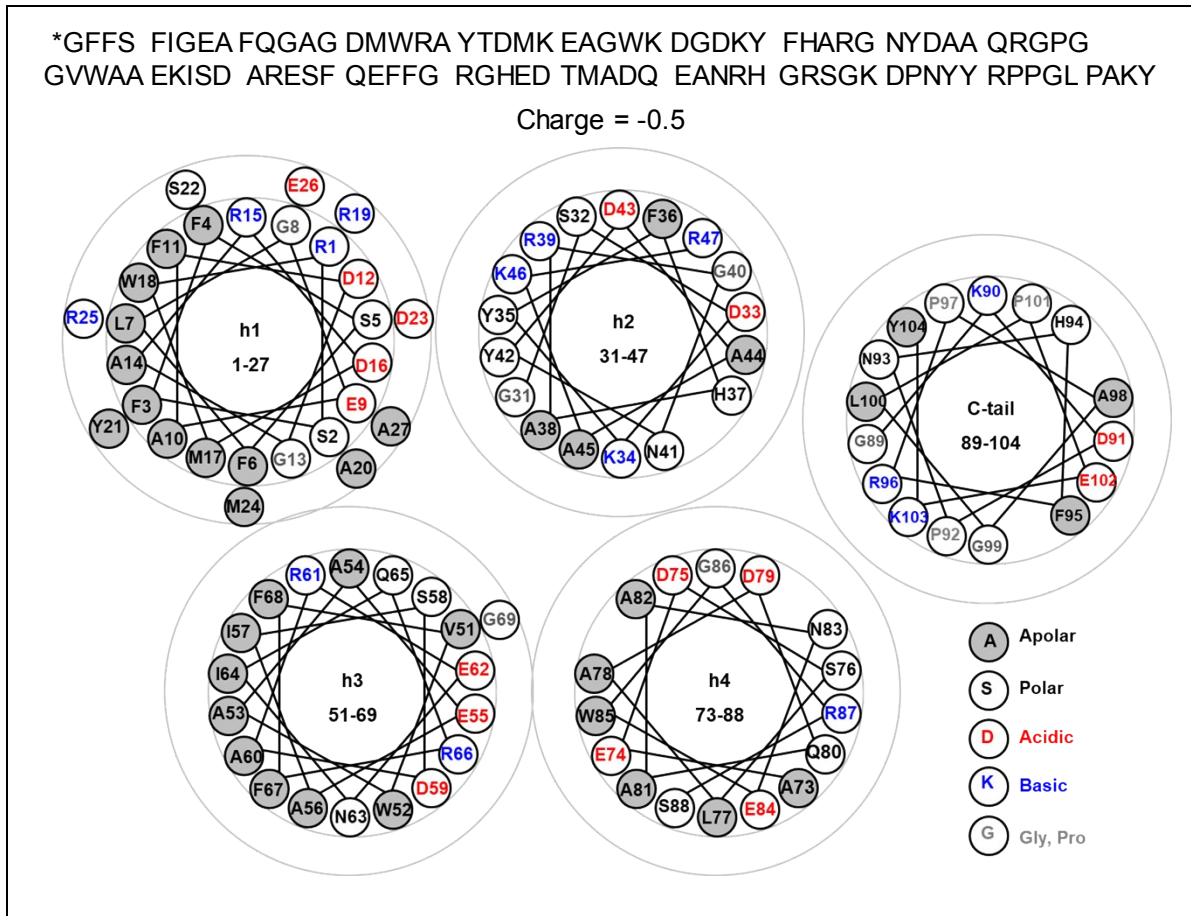


Figure S1. Amino acid sequence and amphipathic properties of mSAA1. The sequence of murine SAA isoform 1.1 that was used in the current study is shown; residue numbering is consistent with hSAA1.1 that contains one additional N-terminal Gly. The protein net charge of -0.5 at pH 7 was predicted on the basis of this sequence by using an on-line server (https://www.ebi.ac.uk/Tools/seqstats/emboss_pepstats/). Helix wheel diagram of residue segments corresponding to helices h1 through h4 from the four-helix bundle seen in the crystal structures of two highly homologous proteins, hSAA1⁶ and mSAA3⁷. The helix wheels clearly show that only helices h1 and h3 in this and all other SAA family proteins are amphipathic and have a high hydrophobic moment, which is characteristic of lipid surface-binding motives. In the crystal structures, the apolar faces of these helices form a large concave hydrophobic surface which, we propose, binds HDL and enables lipid sequestration to from HDL-size particles by SAA oligomers⁸.

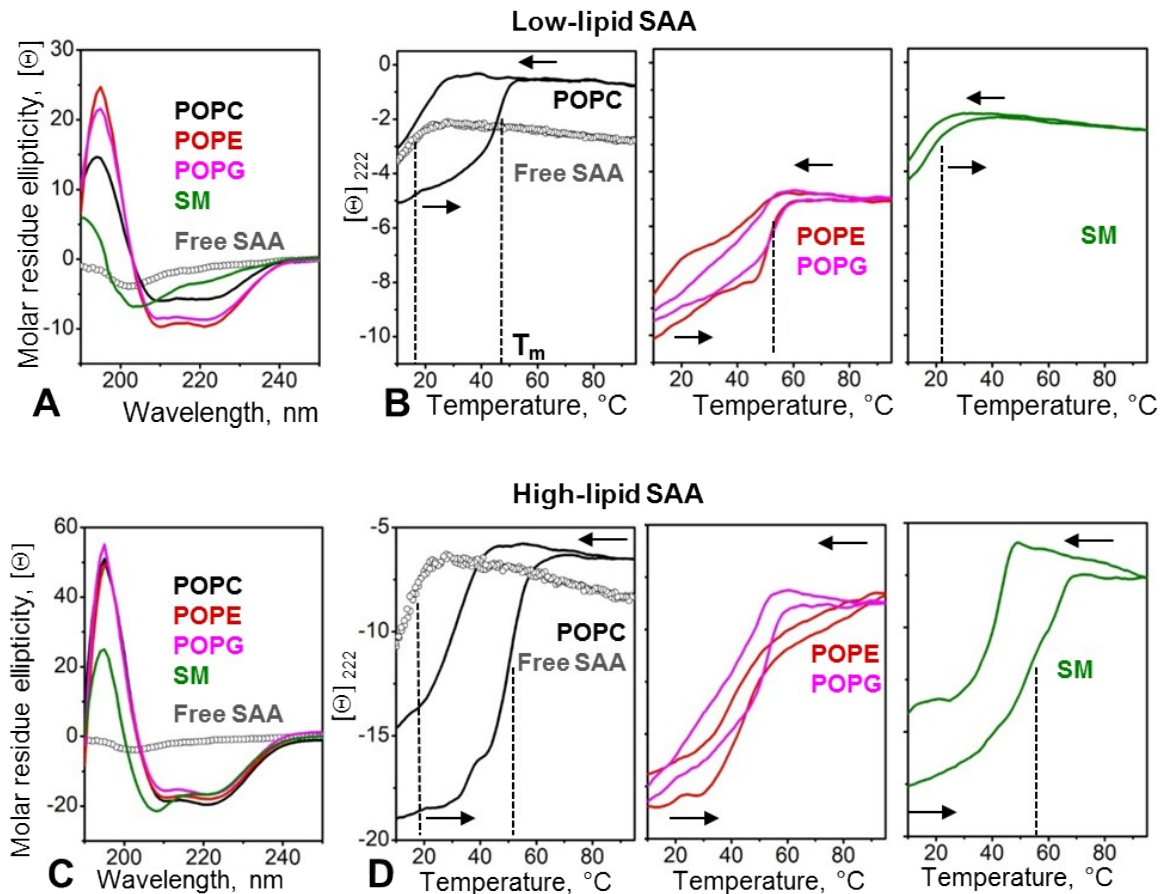


Figure S2. Secondary structural and thermal stability of “low-lipid” (upper panels) and “high-lipid” (lower panels) SAA complexes analyzed by circular dichroism spectroscopy. Far-UV CD spectra at 25 $^{\circ}\text{C}$ (**A**, **C**) and the melting data at 222 nm (**B**, **D**) were recorded as described in Methods and are presented in units of molar residue ellipticity, $[\Theta]$, of $10^3 \cdot \text{deg} \cdot \text{cm}^2 \cdot \text{dmol}^{-1}$. Arrows in the heating and cooling data (panels B, D) show directions of the temperature changes; dotted lines indicate the apparent melting temperatures T_m corresponding to the first derivative maximum of the heating data. Lipids in this and other figures are color-coded: POPC (black), POPE (off-red), POPG (purple), SM (green). The spectrum and the melting data of lipid-free SAA are shown for comparison.

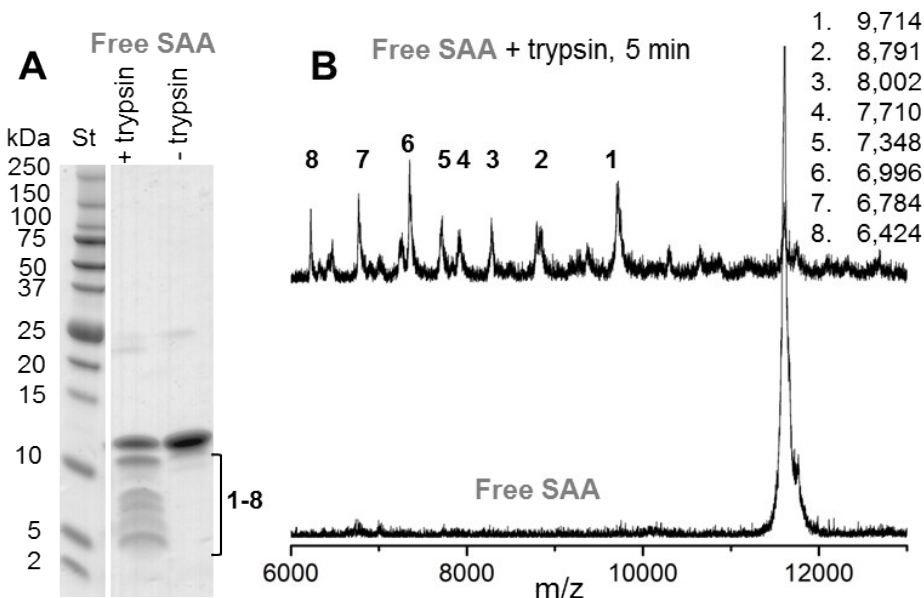


Figure S3. Limited tryptic digestion of lipid-free SAA. SDS PAGE (18%, Denville blue protein stain) (A) and MALDI-TOF mass spectrometry (B) of free SAA before and after tryptic digestion, which was performed for 5 min at 25 °C using 0.5 mg/mL SAA and 1:1500 enzyme:SAA weight ratio as described in Methods. Tryptic fragments 1-8 are numbered and their mass in Da is indicated. Intact free protein, which shows single peak with 11,604 Da, is shown for comparison.

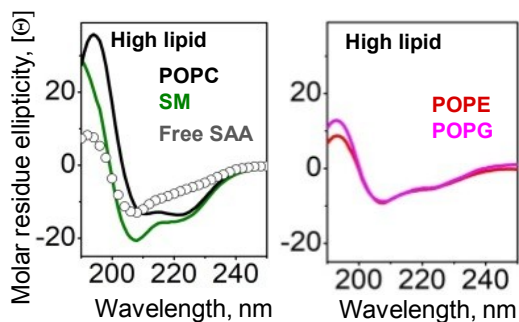


Figure S4. Secondary structural changes in SAA upon incubation at 37 °C for 72 h. In fibrillation studies, SAA samples were incubated as described in Fig. 2A, were diluted to 0.1 mg/mL protein, and far-UV CD spectra were recorded at 25 °C. Since large changes in ThT emission were observed only upon incubation of lipid-free and “high-lipid” SAA complexes, far-UV CD data are shown only for these complexes and for free protein. The spectra shown correspond to amyloid-like structure that binds ThT (Fig. 2A).

Figure S5. Free fatty acid produced by spontaneous hydrolysis of lipids in “high-lipid” complexes containing 0.5 mg/ml SAA under fibrillation condition. Fatty acids were quantified at 0-80 h as described in Methods. Error bars represent the standard error of the mean for three independent measurements.

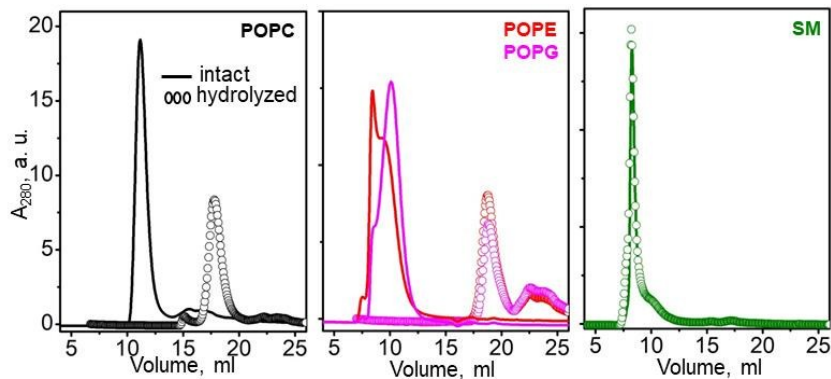
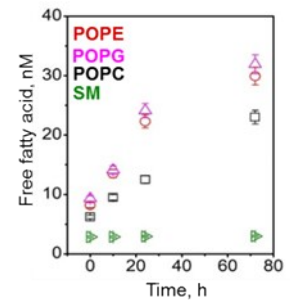


Figure S6. Remodeling of “high-lipid” SAA complex by PLA₂. Size-exclusion chromatography profiles, which were obtained as described in methods using Superdex 75 10/300 GL column, of intact (solid lines) and of PLA₂-hydrolyzed SAA:lipid complexes (open circles). A large shift in the elution volume of hydrolyzed lipoproteins observed in the presence of POPC, POPE, POPG, but not SM (which is not a good substrate for PLA₂) indicates their remodeling by PLA₂ into smaller particles. These results are in excellent agreement with the non-denaturing gel electrophoresis data of these complexes in Fig. 3.

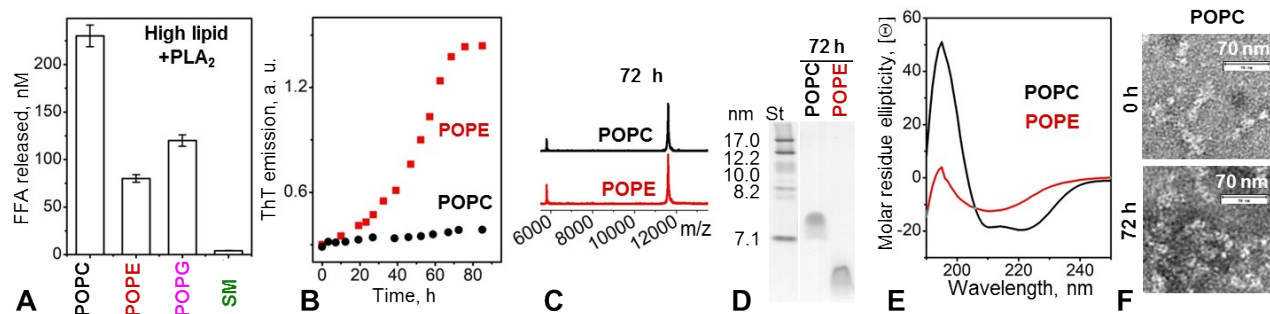


Figure S7. Hydrolysis of “high-lipid” SAA complexes by sPLA₂III and its effects on amyloid formation by SAA. **(A)** Complexes containing 0.5 mg/ml SAA were incubated with sPLA₂III (50 nM) at 37 °C for 3 h. The free fatty acids were quantified as described in Methods. The standard errors of mean for three independent measurements are shown. As a control, MLVs were incubated with the sPLA₂III in the absence of SAA; no free fatty acids were generated, confirming that the hydrolytic activity of the enzyme required lipid surface remodeling. Panels **(B-F)** show data from the “high-lipid” SAA complexes that have been hydrolyzed by PLA₂. **(B)** Fibrillation kinetics monitored by ThT emission as described in Figure 2A legend. A sigmoidal increase in ThT fluorescence observed in complexes with POPE (red) and POPG (not shown to avoid overlap) indicates formation of amyloid-like structure by SAA, while the absence of changes seen in complexes with POPC (black) and SM (not shown to avoid overlap) suggests the absence of amyloid. **(C)** MALDI-TOF analysis of SAA after incubation of its complexes at 37 °C for 72 h. The absence of fragmentation confirms protein integrity. **(D)** Non-denaturing gel electrophoresis and **(E)** far-UV CD spectra of SAA:POPE and SAA:POPG complexes after incubation at 37 °C for 72 h. The spectra were collected at 25 °C from samples containing 0.1 mg/ml SAA in standard buffer. **(F)** TEM of negatively stained complexes; the images were taken before (0 h) and after incubation at 37 °C for 72 h (72 h).

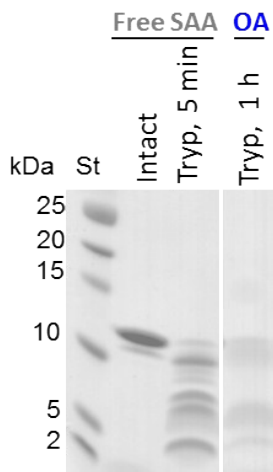


Figure S8. Limited proteolysis of SAA that has been incubated with OA followed by tryptic digestion for 1 h as described in Methods. The protein was analyzed by SDS PAGE (18%, Denville blue protein stain). The gel also shows intact lipid-free SAA and lipid-free SAA that has been digested by trypsin for 5 min.

References

1. Kollmer, M., K. Meinhardt, C. Haupt, F. Liberta, M. Wulff, J. Linder, L. Handl, L. Heinrich, C. Loos, M. Schmidt, T. Syrovets, T. Simmet, P. Westermark, G.T. Westermark, U. Horn, V. Schmidt, P. Walther, and M. Fändrich, *Proc. Natl. Acad. Sci. USA*, 2016, **113(20)**, 5604
2. Patke, S., S. Srinivasan, R. Maheshwari, S.K. Srivastava, J.J. Aguilera, W. Colón and R.S. Kane, *PLoS One*, 2013, **8(6)**, e64974
3. Jayaraman, S., C. Haupt, and O. Gursky, *J. Lipid Res.*, 2015, 56(8), 1531
4. Wang, L. and W. Colón, *Protein Sci.*, 2005 **14(7)**, 1811
5. Jayaraman, S., D.L. Gantz, C. Haupt and O. Gursky. *Proc. Natl. Acad. Sci. USA*, 2017 **114(32)**, E6507
6. Lu, J., Y. Yu, I. Zhu, Y. Cheng and P.D. Sun, *Proc. Natl. Acad. Sci. USA*, 2014, **111(14)**, 5189
7. Derebe, M.G., C.M. Zlatkov, S. Gattu, K.A. Ruhn, S. Vaishnava, G.E. Diehl, J.B. MacMillan, N.S. Williams and L.V. Hooper, *Elife*, 2014, **3**, e03206
8. Frame, N. M. and O. Gursky, *FEBS Lett.*, 2016, **590**, 866